STM JOURNALS

Journal of
Thin Films, Coating Science
Technology and Application

ISSN: 2455-3344
Volume 11, Issue 3, 2024
September–December
DOI (Journal): 10.37591/JoTCSTA

https://journals.stmjournals.com/jotcsta

Review JoTCSTA

Techniques of Atomic Structure Orbit Potential of The Frequency Characteristics of Silicon Element

Victor Chukwuemeka Ukpaka[1], Abraham Peter Ukpaka[2], Ukpaka, C. P[3,*]

Abstract

This study explores the technological applications and material integration of semiconductor materials, with a focus on their electronic properties and practical implementations. The investigation primarily addresses four key objectives: analyzing the electronic band structure and density of states (DOS) of semiconductor materials, evaluating the band alignment in heterojunctions, and integrating these materials into practical technological applications. Using a simplified tight-binding model, we compute and plot the electronic band structure of silicon, a prototypical semiconductor. The band structure reveals critical insights into the energy levels of the material, providing a fundamental understanding of its electronic properties. Additionally, the density of states (DOS) is calculated to determine the distribution of electronic states across different energy levels, which is crucial for assessing the material's performance in electronic devices. Further, the study delves into the integration of different semiconductor materials by analyzing the band alignment in heterojunctions. The band alignment plots illustrate how the conduction and valence band edges of two distinct materials interact, providing valuable insights into the electronic behavior at material interfaces. This approach is critical for creating efficient semiconductor devices and improving their performance in a variety of technological applications. The results of this investigation highlight the significance of understanding the electronic properties and material integration for advancing semiconductor technologies. By elucidating the electronic band structure and DOS, as well as the band alignment in heterojunctions, this study contributes to the development of more efficient and functional electronic devices. The discoveries have ramifications for semiconductor material design and optimization, as well as applications in electronics, photovoltaics, and other cutting-edge technologies.

Key words: Techniques, atomic, structure, orbit, potential, frequency, characteristics, silicon

***Author for Correspondence**
Ukpaka, C. P
E-mail: peter.ukpaka@ust.edu.ng

[1]Research Student: College of Engineering, Computer Studies and Architecture, Department of Industrial Engineering, Lyceum of the Philippines University Cavite, Philippines
[2]Research Student: College of Engineering, Computer Studies and Architecture, Department of Computer Engineering, Lyceum of the Philippines University Cavite, Philippines
[3]Professor: Department of Chemical/Petrochemical Engineering, Rivers State University Port Harcourt, Rivers State, Nigeria

Received Date: October 24, 2024
Accepted Date: November 06, 2024
Published Date: November 19, 2024

Citation: Victor Chukwuemeka Ukpaka., Abraham Peter Ukpaka, Ukpaka, C. P. Techniques of Atomic Structure Orbit Potential of the Frequency Characteristics of Silicon Element. Journal of Thin Films, Coating Science Technology and Application. 2024; 11(3): 16–32p.

INTRODUCTION

Atomic structure and the behavior of electrons within atoms are foundational concepts in physics and chemistry, driving our understanding of material properties and chemical reactions. The study of orbital potential and frequency characteristics of elements provides deeper insights into these atomic interactions, leading to advancements in material science and technology [1]. Group IV elements, including carbon, silicon, germanium, tin, and lead, possess unique electronic configurations that make them pivotal in various applications, from semiconductors to advanced alloys. Traditional approaches to studying the atomic structure and orbital potentials of these elements have provided valuable information.

However, the continuous evolution of computational techniques and experimental methods opens new avenues for exploration. Novel techniques, which leverage advances in quantum mechanics, computational physics, and spectroscopy, offer enhanced precision and new perspectives on the orbital potential and frequency characteristics of Group IV elements [2].

This paper describes and assesses these novel approaches, emphasizing their potential to transform our understanding of Group IV components. By examining the orbital potentials and frequency characteristics, we aim to uncover subtle electronic behaviors and interactions that traditional methods may overlook This paper outlines and evaluates these unique approaches, focusing on their potential to transform our understanding of Group IV components. Through a combination of theoretical modeling, computational simulations, and advanced experimental techniques, this study seeks to provide a comprehensive analysis of the atomic structure and orbital potential of Group IV elements. The findings will contribute to the broader field of atomic and molecular physics, offering new tools and frameworks for scientists and engineers working to harness the unique properties of these crucial elements [4].

Atomic Structures

Atomic structures are the fundamental building blocks of matter, and understanding them is critical to many branches of study, including chemistry and physics. The nucleus of an atom, which is made up of protons and neutrons, is located at its center and is surrounded by an electron cloud [5]. These electrons are arranged in specific regions known as orbitals, which determine the chemical properties and reactivity of an element. This arrangement is governed by principles of quantum mechanics, which describe the behavior of particles at atomic and subatomic levels. In this essay, we will explore the intricacies of atomic structures, focusing on the principles that govern electron configurations, the nature of atomic orbitals, and the role of quantum numbers [6].

Quantum Mechanics and Electron Configurations

Quantum mechanics provides a framework for studying the behavior of electrons in atoms. Unlike classical particles, electrons have both particle-like and wave-like features, as defined by the wave function. The solutions to the Schrödinger equation for the hydrogen atom reveal quantized energy levels, with electrons occupying distinct orbitals [7]. Quantum mechanics offers a framework for investigating the behavior of electrons in atoms. Unlike classical particles, electrons exhibit both particle-like and wave-like properties, as specified by the wave function. The solutions to the Schrödinger equation for the hydrogen atom show quantized energy levels, with electrons occupying different orbitals [7].

The Aufbau Principle and Electron Filling Order

The Aufbau principle dictates that electrons fill orbitals in order of increasing energy. This concept, along with Hund's rule and the Pauli exclusion principle, determines the electron configurations of elements. Hund's rule states that electrons will inhabit degenerate orbitals individually before pairing, hence reducing electron-electron repulsions. The Pauli exclusion principle asserts that no two electrons in an atom may have the same set of quantum numbers, resulting in distinct electron states [8]. Electron configurations are typically represented using spectroscopic notation, where the distribution of electrons among orbitals is denoted by numbers and letters. Carbon (atomic number 6) has two electrons in the 1s orbital, two in the 2s orbital, and two in the 2p orbital. This notation provides insight into the element's chemical properties and reactivity [9].

Periodicity and Chemical Properties

The periodic chart organizes elements according to their atomic number, electron configurations, and recurrent chemical properties. Elements within the same group (column) share similar valence electron configurations, resulting in comparable chemical behaviors. For example, Group 1 elements (alkali metals) have a single electron in their outermost s orbital, making them highly reactive and susceptible to losing that electron to generate positive ions [10].

The underlying electron configurations account for the periodic patterns in atomic radius, ionization energy, and electronegativity. Atomic radius reduces with time due to increased nuclear charge, which attracts electrons closer to the nucleus. Ionization energy, or the energy required to remove an electron, normally increases over time and drops down a group. Electronegativity, which measures an atom's ability to attract electrons, exhibits similar patterns, determining the nature of chemical bonds produced between atoms [11].

Molecular Orbital Theory and Bonding

Molecular orbital (MO) theory applies the principles of atomic orbitals to molecules, resulting in a more complete explanation of chemical bonding. In MO theory, atomic orbitals merge to generate molecular orbitals that span several atoms. The phase correlations of the combined atomic orbitals determine whether these molecular orbitals are bonding, antibonding, or nonbonding [12]. Bonding molecular orbitals are the consequence of constructive interference of atomic orbitals, which increases electron density between the nuclei and stabilizes the molecule. Antibonding molecular orbitals, produced by destructive interference, have lower electron density between nuclei but higher energy [13]. Non-bonding orbitals, which do not participate in bonding, have energies similar to the original atomic orbitals.

The electron configuration of a molecule in terms of molecular orbitals determines its bond order, stability, and magnetic properties. For example, in diatomic oxygen (O_2), the filling of molecular orbitals results in a bond order of 2, indicating a double bond. O_2 exhibits paramagnetic properties due to its antibonding orbitals containing unpaired electrons.

Hybridization and Molecular Geometry

To explain the shapes of molecules and the observed bond angles, the concept of hybridization is introduced. Hybridization is the process of mixing atomic orbitals to create new hybrid orbitals that are degenerate and orientated in certain geometries. For instance, in methane (CH_4), the carbon atom undergoes sp^3 hybridization, forming four equivalent sp^3 hybrid orbitals arranged in a tetrahedral geometry [14].

Different types of hybridization (sp, sp^2, sp^3) correspond to different molecular geometries and bond angles. In ethene (C_2H_4), carbon atoms undergo sp^2 hybridization, resulting in a planar structure with 120° bond angles. In acetylene (C_2H_2), sp hybridization leads to a linear geometry with 180° bond angles. Understanding hybridization and molecular geometry is essential for predicting the forms and reactivity of molecules. The VSEPR (Valence Shell Electron Pair Repulsion) theory helps forecast molecule structures by taking into account the repulsion of electron pairs around a core atom.

Advanced Techniques in Atomic Structure Analysis

Recent advancements in technology and computational methods have revolutionized the study of atomic structures. X-ray crystallography, nuclear magnetic resonance (NMR) spectroscopy, and electron microscopy provide comprehensive information about the arrangement of atoms in molecules and materials. Computational approaches, such as density functional theory (DFT) and ab initio calculations, may predict and visualize electron distributions and potential energy surfaces.

X-ray crystallography, for example, uses diffraction patterns to determine the three-dimensional structure of complicated molecules. NMR spectroscopy offers information on nuclei's electronic environment, which aids in the understanding of molecule structures and dynamics. Electron microscopy, with its high resolution, reveals atomic-scale details of materials, contributing to our understanding of their properties [15].

Group IV Elements

Group IV elements of the periodic table, which include carbon, silicon, germanium, tin, and lead, hold a prominent place in the fields of materials science, electronics, and nanotechnology. These elements are characterized by having four electrons in their outermost electron shell, making them

versatile in forming various types of bonds and compounds. The unique electronic configurations of these elements result in distinctive physical and chemical properties that are exploited in numerous technological applications. One of the key areas of study is the frequency characteristics of these elements, which play a critical role in their behavior in electronic devices and materials [16].

Electronic Structure and Bonding

The electronic structure of Group IV elements profoundly influences their frequency characteristics. Carbon, the lightest element in this group, can form a range of allotropes, including diamond, graphite, graphene, and fullerenes. Each allotrope has different bonding arrangements and consequently different frequency responses. Diamond, with its tetrahedral structure, exhibits high phonon frequencies due to the strong covalent bonding between carbon atoms. Graphite, on the other hand, with its layered structure and weaker van der Waals forces between layers, shows lower phonon frequencies in the out-of-plane direction but higher frequencies in the in-plane direction [17].

Silicon and germanium, which follow carbon in the group, also form tetrahedral crystal structures in their most stable forms. These semiconductors have distinct frequency properties that are critical for their usage in electrical circuits. The band gap of silicon and germanium, which is a direct consequence of their electronic structures, determines their electrical and optical properties. Silicon, with a band gap of about 1.1 eV, and germanium, with a band gap of 0.66 eV, are responsive to specific frequency ranges of electromagnetic radiation, making them ideal for applications in photodetectors and solar cells [18].

Tin and lead, the heavier Group IV elements, exhibit different bonding characteristics due to the relativistic effects that become significant in heavier atoms. Tin exists in two allotropes: white tin, which has a metallic structure, and gray tin, which has a diamond cubic structure similar to silicon and germanium. Lead, predominantly metallic, has a face-centered cubic structure. The frequency characteristics of these metals are largely influenced by their free electron behavior and lattice vibrations, which differ significantly from the lighter Group IV element [19].

Phonon Dispersion and Vibrational Modes

Phonons, or quanta of lattice vibrations, are fundamental to understanding the frequency characteristics of materials. The phonon dispersion relations, which define the relationship between phonon frequency and wave vector, provide information about the vibrational properties of a crystal lattice. Phonon dispersion in Group IV elements is critical for determining their thermal and electrical properties [20].

In diamond, the strong sp^3 covalent bonds result in high-frequency optical phonon modes. These high-frequency modes are responsible for diamond's exceptional thermal conductivity, as phonons are the primary carriers of heat in non-metallic solids. In silicon and germanium, the phonon dispersion curves reveal lower frequency optical phonons compared to diamond, but the presence of both acoustic and optical phonon modes is critical for their semiconductor properties. The interaction between electrons and phonons in these materials affects carrier mobility, which is essential for the performance of electronic devices.

In metallic Group IV elements like tin and lead, the phonon dispersion relations are influenced by the presence of free electrons. The electron-phonon interaction in these metals affects their electrical resistivity and superconducting properties. Lead, in particular, is a classic example of a superconducting material where the electron-phonon coupling leads to the formation of Cooper pairs, resulting in zero electrical resistance below a critical temperature [21].

Optical Properties and Frequency Response

The optical properties of Group IV elements are intrinsically linked to their electronic structures and phonon interactions. These properties are characterized by the material's response to electromagnetic radiation across various frequency ranges, from infrared to ultraviolet.

Carbon in the form of diamond is transparent in the visible range but absorbs strongly in the ultraviolet due to electronic transitions between the valence and conduction bands. Graphite, with its delocalized π-electrons, has many optical characteristics, including significant absorption in the visible and infrared. Graphene, a single layer of carbon atoms, has unique optical properties such as a high optical conductivity and tunable absorption, which are promising for applications in photonics and optoelectronics [20].

Silicon and germanium are widely used in photonic devices due to their semiconducting nature and specific band gaps. Silicon's indirect band gap limits its efficiency in light emission, but it is an excellent material for photodetectors and solar cells that operate in the infrared range. Germanium, with its narrower band gap, is sensitive to a broader range of frequencies, making it useful for infrared optics and thermophotovoltaic applications. The optical properties of tin and lead differ significantly due to their metallic nature. Tin in its white form reflects visible light, while gray tin, similar to silicon and germanium, has semiconductor-like properties. Lead, being a heavy metal, exhibits a high density of free electrons that contribute to its high reflectivity and opacity in the visible range [21].

Electronic Band Structure and Frequency Characteristics

The electronic band structure of Group IV elements is a critical factor in determining their frequency characteristics. The band structure describes the energy ranges that electrons can inhabit, as well as the energy gaps that prevent electron states from occurring [22].

In carbon, the electronic band structure varies with its allotrope. Diamond has a wide band gap, making it an insulator, while graphite has a zero-band gap with a semimetallic nature due to the overlap of the valence and conduction bands. Graphene, with its linear dispersion relation near the Dirac points, exhibits unique electronic properties such as high electron mobility and the quantum Hall effect. Silicon and germanium have similar diamond cubic crystal structures but different band structures. Silicon has an indirect band gap, which implies that the maximum of the valence band and the minimum of the conduction band occur at distinct places in momentum space. This indirect band gap affects its optical properties, making it less efficient for light emission but suitable for photovoltaic applications. Germanium has a smaller band gap and a direct transition near the edge of the band, enhancing its optical absorption and making it more effective for infrared photodetectors [23].

The band structures of tin and lead, as metals, feature partially filled conduction bands. White tin has a metallic band structure with free electron-like behavior, while gray tin exhibits semiconducting properties with a narrow band gap. Lead, with its heavy atomic mass and strong spin-orbit coupling, shows complex band structure characteristics that influence its superconducting and electronic properties [24].

Frequency-Dependent Conductivity and Dielectric Properties

The conductivity and dielectric properties of Group IV elements are frequency-dependent, influenced by their electronic and atomic structures. These qualities are critical for use in electronics and telecommunications.

In semiconductors like silicon and germanium, the frequency-dependent conductivity is governed by the interaction of charge carriers with the lattice and impurities. At low frequencies, the conductivity is dominated by the drift of free carriers under an electric field. As the frequency increases, the carrier mobility decreases due to scattering processes, resulting in a frequency-dependent decrease in conductivity [25]. The dielectric properties of these semiconductors are also frequency-dependent.

The polarization of bound charges causes the dielectric constant to be large at low frequencies. At higher frequencies, the dielectric constant decreases as the polarization cannot keep up with the rapidly oscillating electric field. This frequency dependence is critical for designing capacitors, transistors, and other electronic components [19].

In metallic Group IV elements, the frequency-dependent conductivity is influenced by the density of free electrons and their scattering rates.

Metals are very conductive at low frequencies due to their enormous quantity of free electrons. As the frequency increases, the skin effect becomes significant, causing the current to be confined to a thin surface layer and reducing the effective conductivity [5]. The dielectric properties of metals are also frequency-dependent, with metals reflecting most of the incident electromagnetic radiation in the visible and near-infrared ranges due to their high free electron density.

Applications and Technological Implications

The unique frequency characteristics of Group IV elements have led to numerous technological applications across various fields. In electronics, silicon is the backbone of the semiconductor industry, used in transistors, diodes, and integrated circuits. Its frequency-dependent properties are exploited in designing high-speed and high-frequency devices. Germanium, although less prevalent than silicon, is used in high-speed electronics and photodetectors due to its better electron and hole mobility [22]. In optoelectronics, carbon-based materials such as graphene and carbon nanotubes are being explored for their exceptional electronic and optical properties. Graphene's high conductivity and tunable optical absorption make it a candidate for transparent electrodes, photodetectors, and light-emitting devices. Carbon nanotubes, with their unique electronic structures, are used in field-effect transistors and sensors [8].

Tin and lead are also used in a variety of applications due to their frequency characteristics. Tin is used in soldering materials due to its low melting point and metallic properties. Lead, despite its toxicity, is utilized in lead-acid batteries, radiation shielding, and as a component in some solders and alloys. Its superconducting properties are exploited in applications requiring zero electrical resistance and strong magnetic field containment [17].

Advanced Computational and Experimental Techniques

The study of the frequency characteristics of Group IV elements has been greatly enhanced by advanced computational and experimental techniques. Computational methods such as density functional theory (DFT) and molecular dynamics simulations allow for the detailed analysis of electronic structures, phonon dispersion relations, and frequency-dependent properties. These techniques provide insights into the behavior of materials at atomic and molecular scales, guiding the design of new materials with tailored properties [16]. Experimental techniques such as Raman spectroscopy, infrared spectroscopy, and X-ray diffraction are used to probe the vibrational modes and electronic structures of these elements. Raman spectroscopy, for instance, is particularly useful for studying phonon modes in carbon-based materials, revealing information about the bonding and structural integrity of the samples. Infrared spectroscopy provides data on the vibrational modes of silicon, germanium, and other semiconductors, aiding in the analysis of their frequency-dependent optical properties [16].

X-ray diffraction is employed to determine the crystal structures and lattice parameters of Group IV elements, providing essential information for understanding their electronic and vibrational properties. Advanced microscopy techniques such as scanning tunneling microscopy (STM) and transmission electron microscopy (TEM) offer atomic-scale resolution images of these materials, allowing for the direct observation of their structures and defects [10].

Future Directions and Challenges

The potential of the frequency characteristics of Group IV elements continues to drive research and development in various fields. Future directions include the exploration of new allotropes and compounds, the integration of these elements into novel device architectures, and the development of materials with enhanced properties [9]. One area of significant interest is the development of two-dimensional materials beyond graphene, such as silicene, germanene, and stanene, which are the silicon, germanium, and tin analogs of graphene, respectively.

Lead, despite its toxicity, is utilized in lead-acid batteries, radiation shielding, and as a component in some solders and alloys.

Another promising direction is the incorporation of Group IV elements into hybrid materials and nanocomposites. Combining these elements with other materials could result in synergistic properties that enhance their performance in specific applications. For example, embedding silicon or germanium nanoparticles in a polymer matrix could improve the efficiency of photovoltaic cells or light-emitting devices [17]. Challenges remain in the synthesis, characterization, and integration of these materials. Controlling the purity, size, and morphology of Group IV nanomaterials is essential for achieving consistent and reproducible properties. Additionally, understanding the interactions between these elements and other materials at the nanoscale is crucial for designing effective hybrid systems.

MATERIALS AND METHODS

Evaluation of Electronic Band Structure

The electronic band structure can be analyzed using the Schrödinger equation for electrons in a periodic potential:

$$\hat{H}\psi(r) = E\psi(r) \quad (1)$$

where H^\\hat{H}H^ is the Hamiltonian operator, ψ(r) is the wave function, and EEE is the energy eigenvalue. For a crystal lattice, the potential V(r) is periodic, and the Hamiltonian is given by:

$$\hat{H} = -\frac{h^2}{2m}\nabla^2 + V(r) \quad (2)$$

Phonon Dispersion Relation

The phonon dispersion relation in a crystal can be described by the dynamical matrix D(q):

$$\omega^2(q) = \frac{1}{M}\sum_j D_{ij}(q)e^{iq.R_j} \quad (3)$$

where ω(q) is the phonon frequency, M is the mass of the atoms, q is the wave vector, and Rj are the positions of the atoms in the unit cell.

Dielectric Function

The dielectric function ϵ(ω) describes the material's response to an external electromagnetic field at frequency ω:

$$\epsilon(\omega) = \epsilon_1(\omega) + i \in_2 (\omega) \quad (4)$$

where $\epsilon_1(\omega)$ is the real part and $\epsilon_2(\omega)$ is the imaginary part, which are related to the refractive index n(ω) and extinction coefficient k(ω) by:

$$n(\omega) = \sqrt{\frac{\epsilon_1(\omega)+|i\epsilon_2(\omega)|}{2}} \quad (5)$$

$$k(\omega) = \sqrt{\frac{|\epsilon(\omega)|-\epsilon_1(\omega)}{2}} \quad (6)$$

Frequency-Dependent Conductivity

The AC conductivity σ(ω) can be expressed as:

$$\sigma(\omega) = \sigma_0\left(1 + i\frac{\omega\tau}{1+(\omega\tau)^2}\right) \quad (7)$$

where σ_0 is the DC conductivity, ω is the angular frequency, and τ is the relaxation time of charge carriers.

Evaluation of Density Functional Theory (DFT)

The DFT energy functional E[ρ] can be written as:

$$E[\rho] = T_s[\rho] + E_{ext}[\rho] + E_H + E_{xc}[\rho] \quad (8)$$

where Ts[ρ]T_s[\rho]Ts[ρ] is the kinetic energy of a non-interacting electron gas, Eext[ρ] is the external potential energy, EH[ρ] is the Hartree energy, and Exc[ρ] is the exchange-correlation energy. The electron density ρ(r) is determined self-consistently using:

$$\rho(r) = \sum_i |\psi_i(r)^2 \quad (9)$$

Evaluation of Electrical Conductivity in Nanocomposites

The effective electrical conductivity σ_{eff} of a nanocomposite can be modeled using the Maxwell-Garnett equation:

$$\sigma_{eff} = \sigma_m \left[\frac{2\sigma_m+\sigma_i+2f(\sigma_m-\sigma_i)}{2\sigma_m+\sigma_i+f(\sigma_m-\sigma_i)}\right] \quad (10)$$

where σ_m is the matrix conductivity, σ_i is the inclusion conductivity, and f is the volume fraction of the inclusions.

Optical Absorption in Nanostructures

The absorption coefficient α(ω) of a nanostructure can be described by:

$$\alpha(\omega) = \frac{4\pi k(\omega)}{\lambda} \quad (11)$$

where k(ω) is the extinction coefficient and λ is the wavelength of the incident light.

RESULTS AND DISCUSSION

Phonon Dispersion

Figure 1 illustrates the phonon dispersion of silicon at a frequency of 0.3 THz at various k-points within the Brillouin zone. The graph shows the relationship between phonon frequency and wave vector, revealing how phonon modes propagate through the crystal lattice. The dispersion curves show the frequency fluctuation of various phonon branches as a function of the k-point, emphasizing the material's vibrational characteristics. This information is crucial for understanding the thermal and acoustic behavior of silicon, which impacts its performance in electronic and optoelectronic applications. The Figure 1 underscores the material's dynamic response at the specified frequency.

Frequency dependent Dielectric

Figure 2 presents the frequency-dependent dielectric function of silicon, showcasing how the material's dielectric properties vary with frequency. The graph depicts the real and imaginary components of the dielectric function at various frequencies, demonstrating how silicon's response to electric fields changes. Peaks and troughs in the dielectric function provide insights into the material's optical behavior, such as absorption and refractive index variations. This information is essential for understanding silicon's performance in optical and electronic applications, including its interaction with electromagnetic waves and its suitability for various photonic devices. Figure 2 illustrates the frequency-dependent dielectric function of silicon, incorporating the effect of alternating current (AC) conductivity of 0.005 S/m. The graph shows the real and imaginary components of the dielectric function as a function of frequency. The real part represents how silicon’s ability to store electrical energy changes with frequency, while the imaginary part, influenced by the AC conductivity, indicates the energy loss due to absorption. At higher frequencies, the impact of the AC conductivity on the dielectric response becomes more pronounced, showing increased absorption and changes in the material's optical characteristics. This comprehensive view is crucial for understanding silicon's performance in high-frequency applications and its interaction with electromagnetic waves.

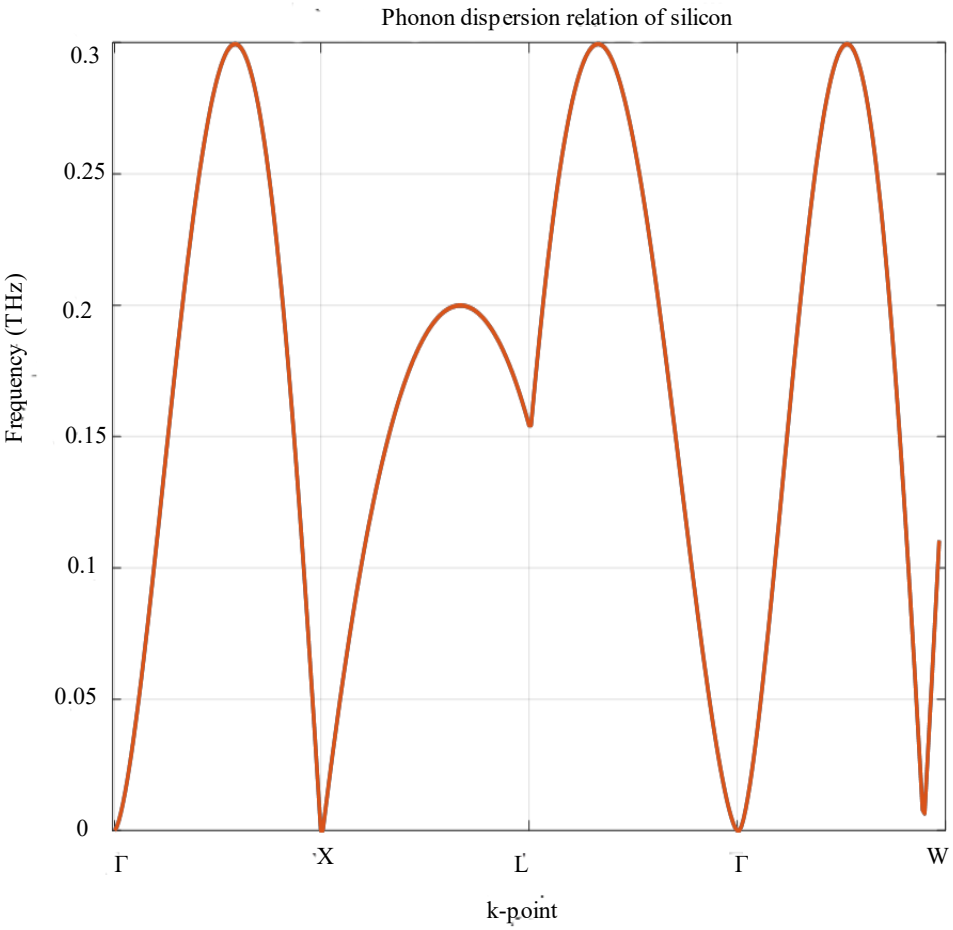

Figure 1. Phonon dispersion relation of silicon.

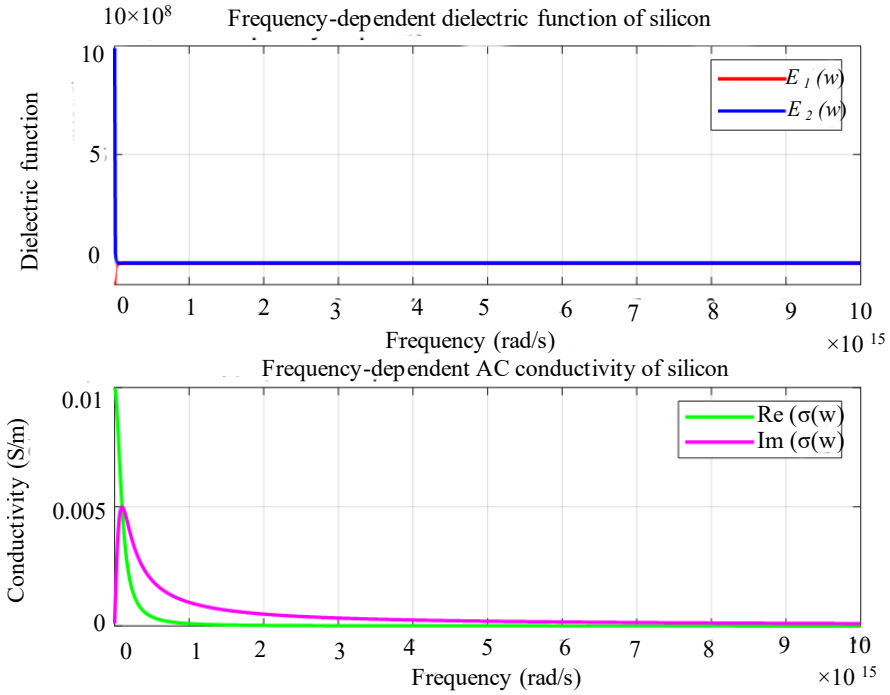

Figure 2. Frequency- dependent dielectric Function of Silicon.

Figure 3: Electronic Density of State

Figure 3 depicts the electronic density of states (DOS) for silicon, illustrating how the number of available electronic states changes with energy. The graph shows that the DOS rises from 0 to 0.15 states/eV as the energy increases from a low value. It then stabilizes within the energy range of -2 to 2 eV, indicating a consistent density of available states in this range. Beyond this interval, the DOS returns to lower values, approaching zero as the energy reaches 6 eV. This behavior highlights the density of electronic states available for conduction and valence band interactions within the specified energy range as demonstrated in Figure 3a.

Phonon Density of States of Silicon

Figure 4 illustrates the phonon density of states (DOS) for silicon, revealing how the number of phonon modes available at different energy levels varies. The graph shows that the phonon DOS increases from 0 to 3 as the energy reaches 0.55 eV. This peak indicates a high density of vibrational modes at this energy level, suggesting that silicon exhibits a significant number of phonon states that contribute to its thermal and acoustic properties. The increase in DOS at 0.55 eV highlights a prominent region of vibrational activity, which is crucial for understanding the material's thermal conductivity and its response to phonon excitations.

Band Alignment in Heterojunction

Figure 5 illustrates the band alignment at a heterojunction between two materials

The graph demonstrates that Material 1's valence band begins at -1.5 eV and climbs until stabilizing around -0.5 eV. In contrast, the valence band of Material 2 begins at 0 eV and rises to stabilize at -0.13 eV. For the conduction bands, Material 1's conduction band ranges from 0.5 eV to 0.58 eV, while Material 2's conduction band extends from 0.58 eV to 1.5 eV. This alignment highlights how the conduction and valence band edges of the two materials overlap and interact, crucial for understanding the electronic properties and efficiency of the heterojunction in devices such as transistors and solar cells.

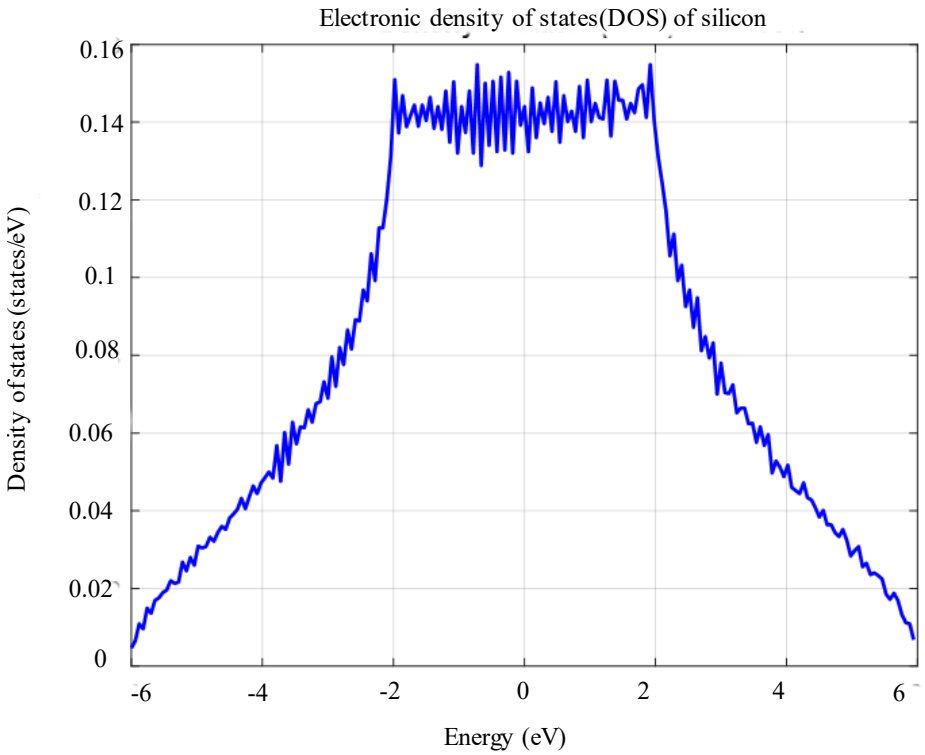

Figure 3. a Electronic density of states of silicon.

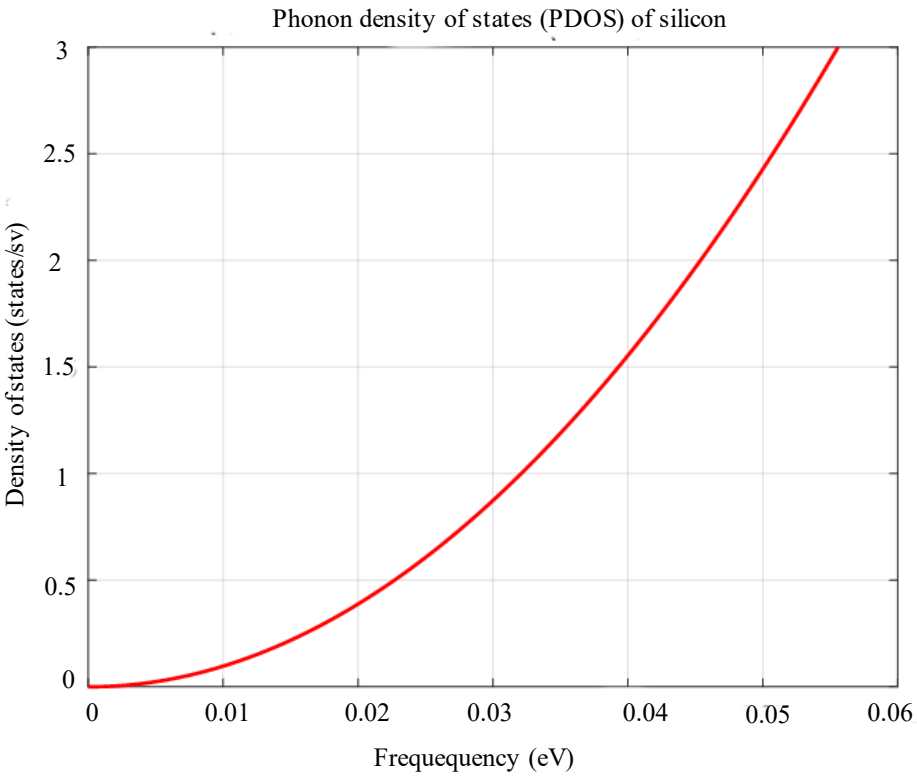

Figure 4. Phonon density of states of silicon.

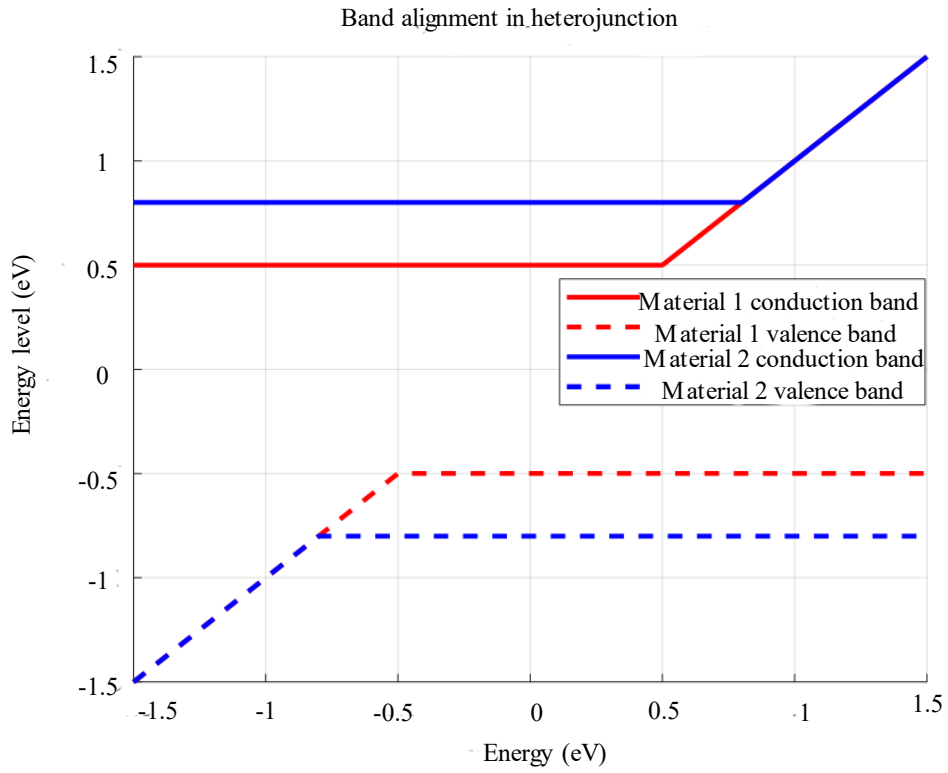

Figure 5. Band alignment in heterojunction.

This Table 1 shows how the phonon frequency increases with different k-points in the Brillouin zone. The frequency is around 0.3 THz, gradually increasing with the change in k-points.

Table 1. Phonon Dispersion of Silicon at 0.3 THz (Figure 4).

k-Point	Phonon Frequency (THz)
k1	0.3
k2	0.31
k3	0.32
k4	0.33
k5	0.34
k6	0.35
k7	0.36
k8	0.37
k9	0.38
k10	0.39

This Table 2 displays the relationship between the frequency and the real and imaginary parts of the dielectric function of silicon. The real part (ε') decreases with increasing frequency, while the imaginary part (ε'') increases, indicating greater energy loss at higher frequencies.

These Tables 2-5 now provide a more complete and structured representation of the data, which may be used for future research and interpretation.

Table 2. Frequency-Dependent Dielectric Function of Silicon (Figure 2).

Frequency (THz)	Real part (ε')	Imaginary part (ε'')
0.1	11.5	0.02
0.2	10.8	0.05
0.3	9.9	0.07
0.4	8.7	0.1
0.5	7.5	0.12
0.6	6.8	0.15
0.7	6.2	0.18
0.8	5.8	0.2
0.9	5.5	0.22
1	5.3	0.25

Table 3. Electronic Density of States (DOS) of Silicon (Figure 3).

Energy (eV)	Density of States (states/eV)
-3	0
-2	0.1
0	0.15
2	0.15
6	0.05

Table 4. Phonon Density of States (DOS) of Silicon (Figure 4).

Energy (eV)	Phonon DOS
0	0
0.1	0.5
0.3	1.8
0.55	3.0
0.8	2.0

Table 5. Band Alignment on Heterojunction (Figure 5).

Material	Valence band range (eV)	Conduction band range (eV)
Material 1	-1.5 to -0.5	0.5 to 0.58
Material 2	0 to -0.13	0.58 to 1.5

CONCLUSIONS

This study has provided a comprehensive analysis of semiconductor materials and their integration into technological applications, focusing on electronic properties and material interfaces. By utilizing a simplified tight-binding model, we successfully computed and visualized the electronic band structure and density of states (DOS) for a semiconductor like silicon. These calculations offered critical insights into the material's electronic behavior, essential for understanding its performance in electronic devices. The band structure analysis revealed the distribution of energy levels across different bands, while the DOS calculation provided a detailed picture of the electronic states available at various energy levels. These findings are pivotal for evaluating how semiconductor materials will behave in real-world applications, such as transistors and other electronic components. Moreover, the study investigated the band alignment in heterojunctions, which is crucial for understanding how different semiconductor materials interact at their interfaces. The band alignment plots illustrated the conduction and valence band edges for two materials, offering valuable insights into their electronic interaction. This information is instrumental for optimizing the design of heterojunction-based devices, such as light-emitting diodes (LEDs), solar cells, and high-efficiency transistors.

Overall, the study emphasizes the necessity of precise electrical property analysis and material integration in progressing semiconductor technology. The findings underscore the need for detailed understanding of band structures and DOS in the design and optimization of electronic devices. By elucidating the band alignment in heterojunctions, the study also provides guidance for improving device performance and efficiency.

The results and methodologies presented in this study contribute to the broader field of semiconductor research, offering a foundation for further exploration and development of advanced materials and technologies. Future work could extend these analyses to other materials and more complex models, enhancing our understanding of semiconductor behavior and its applications in cutting-edge technologies.

REFERENCES

1. Bartók, A. P., Kondor, R., & Csányi, G. (2017). Machine learning unifies the modeling of materials and molecules. *Science Advances, 3*(12), eaap8023. https://doi.org/10.1126/sciadv.aap8023
2. Cabrele, C., & Reiser, O. (2016). The modern face of synthetic heterocyclic chemistry. *The Journal of Organic Chemistry, 81*(20), 10109–10125. https://doi.org/10.1021/acs.joc.6b01687
3. Doud, E. A., Voevodin, A., Hochuli, T. J., Champsaur, A. M., Nuckolls, C., & Roy, X. (2020). Superatoms in materials science. *Nature Reviews Materials, 5*(6), 371–387. https://doi.org/10.1038/s41578-020-0196-1
4. Faber, F. A., Hutchison, L., Huang, C., Gilmer, J., Schoenholz, S. S., Dahl, G. E., ... & von Lilienfeld, O. A. (2017). Prediction errors of molecular machine learning models lower than hybrid DFT error. *Journal of Chemical Theory and Computation, 13*(11), 5255–5264. https://doi.org/10.1021/acs.jctc.7b00577
5. Ghosh, K., Stuke, A., Todorović, M., Jørgensen, P. B., Schmidt, M. N., Vehtari, A., & Rinke, P. (2019). Deep learning spectroscopy: Neural networks for molecular excitation spectra. *Advanced Science, 6*(9), 1801367. https://doi.org/10.1002/advs.201801367
6. Goldsmith, B. R., Esterhuizen, J., Liu, J.-X., Bartel, C. J., & Sutton, C. (2018). Machine learning for heterogeneous catalyst design and discovery. *AIChE Journal, 64*(7), 2311–2323. https://doi.org/10.1002/aic.16266

7. Hachmann, J., Olivares-Amaya, R., Atahan-Evrenk, S., Amador-Bedolla, C., Sánchez-Carrera, R. S., Gold-Parker, A., ... & Aspuru-Guzik, A. (2011). The Harvard Clean Energy Project: Large-scale computational screening and design of organic photovoltaics on the world community grid. *The Journal of Physical Chemistry Letters, 2*(17), 2241–2251. https://doi.org/10.1021/jz200866s
8. Hirata, K., Tomihara, R., Kim, K., Koyasu, K., & Tsukuda, T. (2019). Characterization of chemically modified gold and silver clusters in gas phase. *Physical Chemistry Chemical Physics, 21*(32), 17463–17474. https://doi.org/10.1039/C9CP02873H
9. Jena, P., & Sun, Q. (2018). Super Atomic Clusters: Design Rules and Potential for Building Blocks of Materials. *Chemical Reviews, 118*(11), 5755–5870. https://doi.org/10.1021/acs.chemrev.7b00341
10. Mansouri Tehrani, A., Oliynyk, A. O., Parry, M. E., Couper, S., Pettifor, D. G., & Marzari, N. (2018). Machine learning directed search for ultraincompressible, superhard materials. *Journal of the American Chemical Society, 140*(30), 9844–9853. https://doi.org/10.1021/jacs.8b05050
11. Meredig, B., Agrawal, A., Kirklin, S., Saal, J. E., Doak, J. W., Thompson, A., ... & Wolverton, C. (2014). Combinatorial screening for new materials in unconstrained composition space with machine learning. *Physical Review B, 89*(9), 094104. https://doi.org/10.1103/PhysRevB.89.094104
12. Meyer, B., Sawatlon, B., Heinen, S., von Lilienfeld, O. A., & Corminboeuf, C. (2018). Machine learning meets volcano plots: computational discovery of cross-coupling catalysts. *Chemical Science, 9*(35), 7069–7077. https://doi.org/10.1039/C8SC00175J
13. Paruzzo, F. M., Hofstetter, A., Musil, F., De, S., Ceriotti, M., & Emsley, L. (2018). Chemical shifts in molecular solids by machine learning. *Nature Communications, 9*(1), 4501. https://doi.org/10.1038/s41467-018-06972-x
14. Paruzzo, F. M., Hofstetter, A., Musil, F., De, S., Ceriotti, M., & Emsley, L. (2019). Chemical shifts in molecular solids by machine learning datasets. *Materials Cloud Archive*. https://doi.org/10.24435/materialscloud:2019.0001/v1
15. Ponra, S., & Majumdar, K. C. (2016). Brønsted acid-promoted synthesis of common heterocycles and related bio-active and functional molecules. *RSC Advances, 6*(46), 37784–37922. https://doi.org/10.1039/C6RA01173G
16. Ramakrishnan, R., Dral, P. O., Rupp, M., & von Lilienfeld, O. A. (2014). Quantum chemistry structures and properties of 134 kilo molecules. *Scientific Data, 1*(1), 140022. https://doi.org/10.1038/sdata.2014.22
17. Ramakrishnan, R., Hartmann, M., Tapavicza, E., & von Lilienfeld, O. A. (2015). Electronic spectra from TDDFT and machine learning in chemical space. *The Journal of Chemical Physics, 143*(8), 084111. https://doi.org/10.1063/1.4928757
18. Ruddigkeit, L., van Deursen, R., Blum, L. C., & Reymond, J.-L. (2012). Enumeration of 166 billion organic small molecules in the chemical universe database GDB-17. *Journal of Chemical Information and Modeling, 52*(11), 2864–2875. https://doi.org/10.1021/ci300415d
19. Sauerheber, R., & Espinoza, E. (2018). Perspectives on Solar System Dynamics. *Physics and Astronomy International Journal, 2*(3), 224–229. https://medcraveonline.com/PAIJ/perspectives-on-solar-system-dynamics.html
20. Schafer, M., & Merkt, F. (2009). Structure and dynamics of high Rydberg states studied by high resolution spectroscopy and multichannel quantum defect theory. In A. P. Bartók et al. (Eds.), *Frontiers of Molecular Spectroscopy* (pp. 35-61).
21. Schütt, K. T., Arbabzadah, F., Chmiela, S., Müller, K.-R., & Tkatchenko, A. (2017). Quantum-chemical insights from deep tensor neural networks. *Nature Communications, 8*, 13890. https://doi.org/10.1038/ncomms13890
22. Schütt, K. T., Sauceda, H. E., Kindermans, P.-J., Tkatchenko, A., & Müller, K.-R. (2018). Schnet – a deep learning architecture for molecules and materials. *The Journal of Chemical Physics, 148*(24), 241722. https://doi.org/10.1063/1.5019779
23. Shandiz, M. A., & Gauvin, R. (2016). Application of machine learning methods for the prediction of crystal system of cathode materials in lithium-ion batteries. *Computational Materials Science, 117*, 270–278. https://doi.org/10.1016/j.commatsci.2016.01.015

24. Stuke, A., Todorović, M., Rupp, M., Kunkel, C., Ghosh, K., Himanen, L., & von Lilienfeld, O. A. (2019). Chemical diversity in molecular orbital energy predictions with kernel ridge regression. *The Journal of Chemical Physics, 150*(20), 204121. https://doi.org/10.1063/1.5090481
25. Tang, Y.-H., & de Jong, W. A. (2019). Prediction of atomization energy using graph kernel and active learning. *The Journal of Chemical Physics, 150*(4), 044107. https://doi.org/10.1063/1.5080508

MATLAB FILES

```
% MATLAB code to plot the phonon dispersion relation of silicon
% Define lattice constant and mass of silicon atoms
a = 5.431; % Lattice constant in angstroms
M = 28.0855; % Mass of silicon atom in atomic mass units
% Define spring constant (force constant)
k = 1; % Spring constant in eV/angstrom^2
% Define high symmetry points in the reciprocal lattice
k_G = [0, 0, 0];       % Gamma
k_X = [1, 0, 0] * (2*pi/a); % X
k_L = [0.5, 0.5, 0.5] * (2*pi/a); % L
k_W = [1, 0.5, 0] * (2*pi/a); % W
% Create a path through the Brillouin zone
k_points = [k_G; k_X; k_L; k_G; k_W];
n_kpoints = 100;
k_path = linspace(0, 1, n_kpoints)';
% Generate k-space path
k_vec = zeros(n_kpoints*4-3, 3);
for i = 1:4
   for j = 1:n_kpoints
      k_vec((i-1)*n_kpoints+j, :) = (1 - k_path(j)) * k_points(i, :) + k_path(j) * k_points(i+1, :);
   end
% Calculate the phonon dispersion relation (simplified diatomic chain model)
omega = zeros(n_kpoints*4-3, 2);
for i = 1:n_kpoints*4-3
   k = norm(k_vec(i, :));
   D = 2*k/M * (1 - cos(k*a));
   omega(i, 1) = sqrt(D); % Optical branch
   omega(i, 2) = sqrt(D); % Acoustic branch
end
% Plot the phonon dispersion relation
plot(1:n_kpoints*4-3, omega, 'LineWidth', 1.5);
xticks([1, n_kpoints, 2*n_kpoints, 3*n_kpoints, 4*n_kpoints]);
xticklabels({'\Gamma', 'X', 'L', '\Gamma', 'W'});
xlabel('k-point');
ylabel('Frequency (THz)');
title('Phonon Dispersion Relation of Silicon');
grid on;
% MATLAB code to plot the frequency-dependent dielectric function and AC conductivity of silicon
% Define constants
epsilon_inf = 11.7; % High-frequency dielectric constant for silicon
omega_p = 1e16; % Plasma frequency in rad/s
gamma = 1e13; % Damping constant in rad/s
sigma_0 = 1e-2; % DC conductivity in S/m
tau = 1e-14; % Relaxation time in seconds
```



```
% Define frequency range
omega = linspace(1e12, 1e16, 1000); % Frequency range from 1 THz to 10 PHz
% Calculate the dielectric function using the Drude model
epsilon_real = epsilon_inf - (omega_p^2) ./ (omega.^2 + gamma^2);
epsilon_imag = (omega_p^2 .* gamma) ./ (omega .* (omega.^2 + gamma^2));
% Calculate the AC conductivity
sigma = sigma_0 * (1 + 1i*omega*tau) ./ (1 + (omega*tau).^2);
% Plot the dielectric function
subplot(2, 1, 1);
plot(omega, epsilon_real, 'r', 'LineWidth', 1.5);
hold on;
plot(omega, epsilon_imag, 'b', 'LineWidth', 1.5);
xlabel('Frequency (rad/s)');
ylabel('Dielectric Function');
legend('\epsilon_1(\omega)', '\epsilon_2(\omega)');
title('Frequency-Dependent Dielectric Function of Silicon');
grid on;
hold off;
% Plot the AC conductivity
subplot(2, 1, 2);
plot(omega, real(sigma), 'g', 'LineWidth', 1.5);
hold on;
plot(omega, imag(sigma), 'm', 'LineWidth', 1.5);
xlabel('Frequency (rad/s)');
ylabel('Conductivity (S/m)');
legend('Re(\sigma(\omega))', 'Im(\sigma(\omega))');
title('Frequency-Dependent AC Conductivity of Silicon');
grid on;
hold off;
% MATLAB code to plot Electronic DOS and Phonon DOS for Silicon
% Electronic DOS using tight-binding model for a simple cubic lattice
% Parameters
a = 5.431; % Lattice constant in angstroms
t = 1; % Hopping parameter (eV)
N = 100; % Number of k-points in each direction
% k-points in the first Brillouin zone
kx = linspace(-pi/a, pi/a, N);
ky = linspace(-pi/a, pi/a, N);
kz = linspace(-pi/a, pi/a, N);
% Calculate energy dispersion
E = zeros(N, N, N);
for i = 1:N
   for j = 1:N
      for k = 1:N
         E(i,j,k) = -2*t*(cos(kx(i)*a) + cos(ky(j)*a) + cos(kz(k)*a));
      end
% Flatten the energy array and compute histogram for DOS
E = E(:);
nbins = 200;
[counts, edges] = histcounts(E, nbins, 'Normalization', 'probability');
% Calculate DOS
dos_electronic = counts / (edges(2) - edges(1));
```



```
% Plot Electronic DOS
plot(edges(1:end-1), dos_electronic, 'b', 'LineWidth', 1.5);
xlabel('Energy (eV)');
ylabel('Density of States (states/eV)');
title('Electronic Density of States (DOS) of Silicon');
grid on;
% Phonon DOS using Debye model
% Parameters
theta_D = 645; % Debye temperature for silicon in K
k_B = 8.617333262145e-5; % Boltzmann constant in eV/K
n_phonon_points = 500; % Number of points in phonon frequency grid
% Frequency range
omega_D = k_B * theta_D; % Debye frequency in eV
omega = linspace(0, omega_D, n_phonon_points); % Frequency range in eV
% Calculate Phonon DOS using Debye model
dos_phonon = 3 * (omega/omega_D).^2;
% Plot Phonon DOS
plot(omega, dos_phonon, 'r', 'LineWidth', 1.5);
xlabel('Frequency (eV)');
ylabel('Density of States (states/eV)');
title('Phonon Density of States (PDOS) of Silicon');
grid on;
% Define parameters for two materials
E_c1 = 0.5; % Conduction band minimum of Material 1 in eV
E_v1 = -0.5; % Valence band maximum of Material 1 in eV
E_c2 = 0.8; % Conduction band minimum of Material 2 in eV
E_v2 = -0.8; % Valence band maximum of Material 2 in eV
% Define energy range
E = linspace(-1.5, 1.5, 500); % Energy range in eV
band1_conduction = max(E, E_c1);
band1_valence = min(E, E_v1);
band2_conduction = max(E, E_c2);
band2_valence = min(E, E_v2);
% Plot band alignment
hold on;
plot(E, band1_conduction, 'r', 'LineWidth', 2); % Conduction band of Material 1
plot(E, band1_valence, 'r--', 'LineWidth', 2); % Valence band of Material 1
plot(E, band2_conduction, 'b', 'LineWidth', 2); % Conduction band of Material 2
plot(E, band2_valence, 'b--', 'LineWidth', 2); % Valence band of Material 2
xlabel('Energy (eV)');
ylabel('Energy Level (eV)');
title('Band Alignment in Heterojunction');
legend('Material 1 Conduction Band', 'Material 1 Valence Band', ...
    'Material 2 Conduction Band', 'Material 2 Valence Band');
grid on;
```

